A Discrete-Time Model for Triply Selective MIMO Rayleigh Fading Channels

Chengshan Xiao, *Senior Member, IEEE*, Jingxian Wu, Sang-Yick Leong, Yahong Rosa Zheng, and Khaled Ben Letaief, *Fellow, IEEE*

***Abstract*—A statistical discrete-time model is proposed for simulating wideband multiple-input multiple-output (MIMO) fading channels which are triply selective due to angle spread, Doppler spread, and delay spread. The new discrete-time MIMO channel model includes the combined effects of the transmit filter, physical MIMO multipath channel fading, and receive filter, and it has the same sampling period as that of the MIMO receiver. This leads to very efficient simulation of physical continuous-time MIMO channels. A new method is also presented to efficiently generate the MIMO channel stochastic coefficients. The statistical accuracy of the discrete-time MIMO channel model is rigorously verified through theoretical analysis and extensive simulations in different conditions. The high computational efficiency of the discrete-time MIMO channel model is illustrated by comparing it to that of the continuous-time MIMO channel model. The new model is further employed to evaluate the channel capacity of MIMO systems in a triply selective Rayleigh fading environment. The simulation results reveal some interesting effects of spatial correlations, multipaths, and number of antennas on the MIMO channel capacity.**

***Index Terms*—Discrete-time channel model, multiple-input multiple-output (MIMO) channel, multiple-input multiple-output multipath channel capacity, Rayleigh fading, triply selective fading, wide-sense stationary uncorrelated scattering (WSSUS) multipath channel.**

I. Introduction

THE multiple-input multiple-output (MIMO) communication architecture has recently emerged as a new paradigm for high data rate wireless cellular communications in rich multipath environments. Using multiple-element antenna arrays at both the transmitter and receiver, which effectively exploits the spatial dimension in addition to time and frequency dimensions, this architecture shows channel capacity potential far beyond that of traditional techniques. In quasi-static, independent and identically distributed (i.i.d.) frequency flat Rayleigh fading channels, the MIMO capacity scales linearly with the number of antennas under some conditions [1], [2]. However, in practice, subchannels of a MIMO system are usually space-selective (caused by angle spread at the transmitter and/or receiver), time-selective (caused by Doppler spread), and frequency-selective (caused by delay spread), which are referred to as *triply selective* MIMO channels in this paper. These selectivities may substantially affect the MIMO performance [3], [4]. Further work in this field necessitates a realistic and efficient MIMO channel simulation model to investigate, evaluate, and test new algorithms and performance of MIMO wireless systems under triply selective fading scenarios.

The topic of MIMO channel modeling has received great interest recently [5]–[12]. Frequency-selective Rayleigh fading channels were discussed in [5] and [6] with certain assumptions, while flat Rayleigh fading channels were explored in [12]. Physical channel models which include antenna polarization and/or angular information were discussed in [7]–[11]. But, all of these previous models are special cases of triply selective fading, and they are continuous-time-based models. When the number of multiple delayed fading paths is large and/or the differential delay between paths is small, which is usually true for wideband systems in practice, then a significant amount of computational effort is required in simulations with continuous-time channel models [13].

The discrete-time channel model was first presented by Forney [14], and simulation models in the discrete-time domain were discussed in [15]–[17] for single-input single-output (SISO) wireless channels. These papers [15]–[17] qualitatively showed the computational efficiency in favor of the discrete-time models; however, simulation results showed that these discrete-time models are not statistically equivalent to their continuous-time counterparts. For example, the bit-error rate (BER) performance from these discrete-time models of a mobile communication system is different from that of the corresponding continuous-time models. This significantly reduces the practical value of these simulation models in [15]–[17]. Therefore, an accurate discrete-time model for both SISO and MIMO channels is highly desirable.

The main objective of this paper is to establish a discrete-time MIMO channel model, which is statistically accurate and computationally efficient to characterize the continuous-time MIMO Rayleigh fading channel that is triply selective. The discrete-time MIMO channel model will translate the effects of transmit filter, physical MIMO channel fading, and receive filter into the receiver's sampling-period spaced stochastic channel coefficients. No oversampling is needed to handle multiple fractionally delayed fading paths or to approximate channels with possible continuous delayed paths. The simulation of a MIMO system is carried out in a pure discrete manner, which leads to

Manuscript received October 16, 2002; revised April 4, 2003 and June 6, 2003; accepted June 23, 2003. The editor coordinating the review of this paper and approving it for publication is F.-C. Zheng. The work of K. B. Letaief was supported by HKTIIT. The work of C. Xiao was supported in part by the University of Missouri-Columbia Research Council under Grant URC-02-050 and by the University of Missouri System Research Board under Grant URB-02-0124.

C. Xiao, J. Wu, S.-Y. Leong, and Y. R. Zheng are with the Department of Electrical and Computer Engineering, University of Missouri, Columbia, MO 65211 USA (e-mail: xiaoc@missouri.edu, jwu@ee.missouri.edu; syleong@ee.missouri.edu; yzheng@ee.missouri.edu).

K. B. Letaief is with the Department of Electronic and Electrical Engineering, Hong Kong University of Science and Technology, Hong Kong (e-mail: eekhaled@ee.ust.hk).

Digital Object Identifier 10.1109/TWC.2004.833444

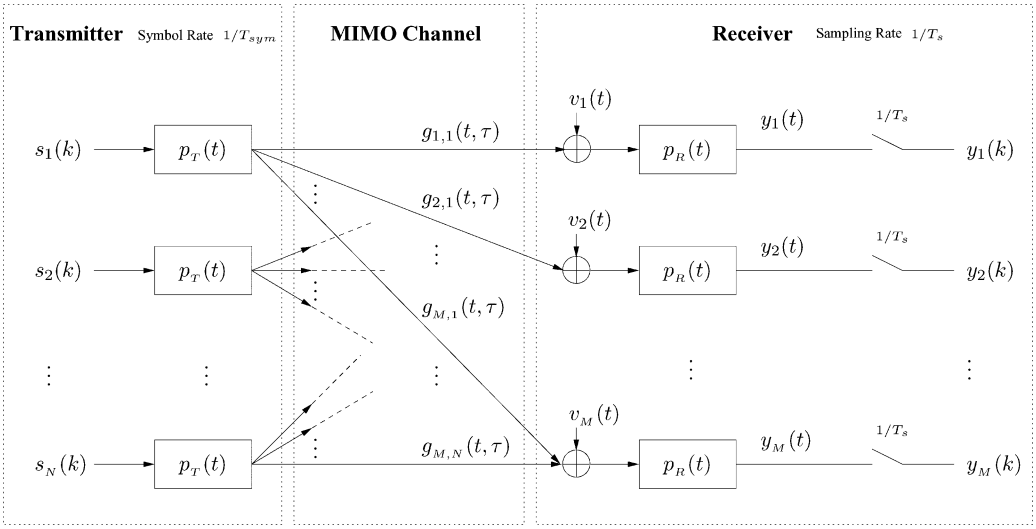

Fig. 1. Conventional continuous-time baseband MIMO channel model.

a higher computational efficiency and possible better statistical accuracy.

This paper is organized as follows. Section II describes the continuous-time MIMO Rayleigh fading channel which includes the transmit filter, physical MIMO fading channel, and receive filter. Two assumptions on the physical MIMO channel are also stated in this section. Section III proposes a discrete-time MIMO channel model which is statistically equivalent to the continuous-time MIMO channel model. The statistical properties of the discrete-time MIMO Rayleigh fading channel are analyzed in detail and further used to generate the stochastic channel coefficients for simulation purposes. Simulation experiments are shown in Section IV to demonstrate the statistical accuracy, computational efficiency, and applications of the discrete-time MIMO channel model, including the evaluation of MIMO channel capacity under triply selective fading scenarios. Finally, Section V concludes the paper.

II. MIMO Channel Description and Assumptions

A. MIMO Channel Description

We consider a wideband MIMO wireless channel which contains N transmit antennas and M receive antennas. Let $p_T(t)$ and $p_R(t)$ be the time-invariant impulse responses of the transmit filter and the receive filter, respectively, and both are normalized with energy of unity. Let $g_{m,n}(t,\tau)$ be the time-varying impulse response of the (m,n)th subchannel connecting the nth transmit antenna and the mth receive antenna, where $g_{m,n}(t,\tau)$ is defined as the response at time t to an impulse applied to the subchannel at time $t-\tau$ [18]. The block diagram of this MIMO channel is depicted in Fig. 1, where $\{s_n(k)\}$ is a sequence of complex symbols transmitted by the nth transmit antenna with symbol period of T_{sym}, $y_m(t)$ is the received signal at the mth receive antenna, and $y_m(k)$ is the sampled version of $y_m(t)$ with sampling period of $T_s = T_{\text{sym}}/\gamma$, and γ is an integer number. If $\gamma = 1$, then the sampling rate at the receiver is the same as the symbol rate at the transmitter.

We define the combined impulse response of the (m,n)th subchannel as

$$h_{m,n}(t,\tau) = p_R(\tau) \odot g_{m,n}(t,\tau) \odot p_T(\tau) \tag{1}$$

where $a(\tau) \odot b(t,\tau) = \int b(t,\alpha)a(\tau-\alpha)d\alpha$ represents the convolution operation. Therefore, the received signal $y_m(t) = \int h_{m,n}(t,\tau)s_n(t-\tau)d\tau$ can be expressed by

$$y_m(t) = \sum_{n=1}^{N}\sum_{k=-\infty}^{\infty} s_n(k)h_{m,n}(t,t-kT_{\text{sym}}) + z_m(t), \quad m = 1,2,\ldots,M \tag{2}$$

where $z_m(t)$ is the additive noise given by

$$z_m(t) = v_m(t) \odot p_R(t) \tag{3}$$

and $v_m(t)$ is the zero-mean complex-valued white Gaussian noise with a two-sided power spectral density N_0. The sampled version of the received signal at the mth receive antenna is given by

$$y_m(kT_s) = \sum_{n=1}^{N}\sum_{l=-\infty}^{\infty} s_n(l)h_{m,n}(kT_s, kT_s - l\gamma T_s) + z_m(kT_s), \quad m = 1,2,\ldots,M. \tag{4}$$

If we oversample the transmitted sequence $\{s_n(k)\}$ by inserting $(\gamma-1)$ zeros between each symbol $s_n(k)$, then the oversampled sequence denoted by $\{x_n(k)\}$ can be defined as

$$x_n(k) = \begin{cases} s_n\left(\frac{k}{\gamma}\right), & \text{if } \frac{k}{\gamma} \text{ is integer} \\ 0, & \text{otherwise.} \end{cases} \tag{5}$$

Replacing $s_n(k)$ in (4) by $x_n(k)$, we obtain the following equation with a single data rate of $1/T_s$

$$y_m(k) = \sum_{n=1}^{N}\sum_{l=-\infty}^{\infty} x_n(k-l)h_{m,n}(k,l) + z_m(k), \quad m = 1,2,\ldots,M \tag{6}$$

where $h_{m,n}(k,l) = h_{m,n}(kT_s, lT_s)$ is the T_s-space sampled version of $h_{m,n}(t,\tau)$, and $z_m(k) = z_m(kT_s)$ is the T_s-space sampled version of $z(t)$.

With the statistical properties of the discrete-time channel coefficients $h_{m,n}(k,l)$ and the additive noises $z_m(k)$, the MIMO channel input–output can be fully characterized in the discrete-time domain with high computational efficiency and no loss of information. Details are given in Section III.

B. MIMO Channel Assumptions

We have two assumptions on the continuous-time physical channel of wideband MIMO wireless systems.

Assumption 1: The (m,n)th subchannel $g_{m,n}(t,\tau)$ of a MIMO system is a wide-sense stationary uncorrelated scattering (WSSUS) [18], [19] Rayleigh fading channel with a zero mean and autocorrelation given by

$$E\left\{g_{m,n}(t,\tau)\cdot g^*_{m,n}(t-\xi,\tau')\right\} = J_0(2\pi f_d\xi)\cdot G(\tau)\cdot\delta(\tau-\tau'),\quad \forall m,n \quad (7)$$

where $(\cdot)^*$ is the conjugate operator, f_d is the maximum Doppler frequency, and $G(\tau)$ is the power delay profile with $\int_{-\infty}^{\infty} G(\tau)d\tau = 1$.

It is important to note that this assumption is commonly employed for SISO channels in the literature [13], [15]–[17] and in wireless standards documents [22], [23] for both TDMA-based global system for mobile (GSM) communications, Enhanced Data rate for Global Evolution (EDGE) systems, and code-division multiple-access (CDMA)-based universal mobile telecommunications systems (UMTS) and cdma2000 systems. Moreover, the power delay profile $G(\tau)$ is often assumed to be discrete and is given by

$$G(\tau) = \sum_{i=1}^{K}\sigma_i^2\delta(\tau-\tau_i) \quad (8)$$

where K is the number of total resolvable paths and σ_i^2 is the power of the ith path with delay τ_i. For example, the typical urban (TU), hilly terrain (HT), and equalization test (EQ) profiles for GSM and EDGE systems [22] as well as the pedestrian and vehicular profiles for channel A and channel B of cdma2000 and UMTS systems [23] have all been defined as discrete delayed Rayleigh fading paths, and almost all the path delays τ_i are not an integer multiple of their system's symbol period T_{sym} (or chip period T_c for CDMA systems).

This assumption implies that the fades of all the subchannels are identically distributed. However, it does not require them to be statistically independent. This implies that the subchannels are not necessarily i.i.d., which was commonly assumed in the literature for MIMO channels.

Assumption 2: The space selectivity or (spatial correlation) between the (m,n)th subchannel $g_{m,n}(t,\tau)$ and the (p,q)th subchannel $g_{p,q}(t,\tau)$ is given by

$$E\left\{g_{m,n}(t,\tau)\cdot g^*_{p,q}(t-\xi,\tau')\right\} = \rho_{Rx}^{(m,p)}\cdot\rho_{Tx}^{(n,q)}\cdot J_0(2\pi f_d\xi)\cdot G(\tau)\cdot\delta(\tau-\tau') \quad (9)$$

where $\rho_{Rx}^{(m,p)}$ is the receive correlation coefficient between receive antennas m and p with $0 \le \left|\rho_{Rx}^{(m,p)}\right| \le \rho_{Rx}^{(m,m)} = 1$, and $\rho_{Tx}^{(n,q)}$ is the transmit correlation coefficient between transmit antennas n and q with $0 \le \left|\rho_{Tx}^{(n,q)}\right| \le \rho_{Tx}^{(n,n)} = 1$.

Assumption 2 is a straightforward extension of the MIMO Rayleigh flat fading case in [24] to the MIMO WSSUS multipath Rayleigh fading case. It implies three subassumptions as explained in [24] and cited as follows: 1) the transmit correlation between the fading from transmit antennas n and q to the same receive antenna does not depend on the receive antenna; 2) the receive correlation between the fading from a transmit antenna to receive antennas m and p does not depend on the transmit antenna; and 3) the correlation between the fading of two distinct transmit-receive antenna pairs is the product of the corresponding transmit correlation and receive correlation. These three subassumptions are actually the "Kronecker correlation" assumption used in the literature, and they are quite accurate and commonly used for MIMO Rayleigh fading channels [4], [25]. However, it should be pointed out that the third subassumption may not be extended to Rice fading MIMO channels [26].

It is noted here that the spatial correlation coefficients $\rho_{Rx}^{(m,p)}$ and $\rho_{Tx}^{(n,q)}$ are determined by the spatial arrangements of the transmit and receive antennas, and the angle of arrival, the angular spread, etc. They can be calculated by mathematical formulas [4], [25] or obtained from experimental data.

III. Discrete-Time MIMO Channel Model

In this section, we present a discrete-time model for triply selective MIMO Rayleigh fading channels, then we investigate the statistical properties of this MIMO channel in the discrete-time domain. These statistics are further used to build a computationally efficient discrete-time MIMO channel simulator, which is equivalent to its counterpart in the continuous-time domain in terms of various statistic measures.

A. Discrete-Time Channel Model

It is known that the total number of T_s-spaced discrete-time channel coefficients $h_{m,n}(k,l)$ is determined by the maximum delay spread of the physical fading channel $g_{m,n}(t,\tau)$ and the time durations of the transmit filter and receive filter, which are usually infinite in theory to maintain limited frequency bandwidth. Therefore, $h_{m,n}(k,l)$ is normally a time-varying noncausal filter with infinite impulse response (IIR).[1] However, in practice, the time-domain tails of the transmit and receive filters are designed to fall off rapidly. Thus, the amplitudes of the channel coefficients $h_{m,n}(k,l)$ will decrease quickly with increasing $|l|$. When the power (or squared amplitude) of a coefficient is smaller than a predefined threshold, for example, 0.01% of the total power of its corresponding subchannel, it has very little impact on the output signal and thus can be discarded. Therefore, the time-varying noncausal IIR channel can be truncated to a finite impulse response (FIR) channel. Without loss of generality, we assume that the coefficient index l is in the range of $[-L_1, L_2]$, where L_1 and L_2 are nonnegative

[1]It should be noted that the noncausality of $h_{m,n}(k,l)$ is induced by the effects of the transmit filter and receive filter, while the physical CIR $g_{m,n}(t,\tau)$ is always causal.

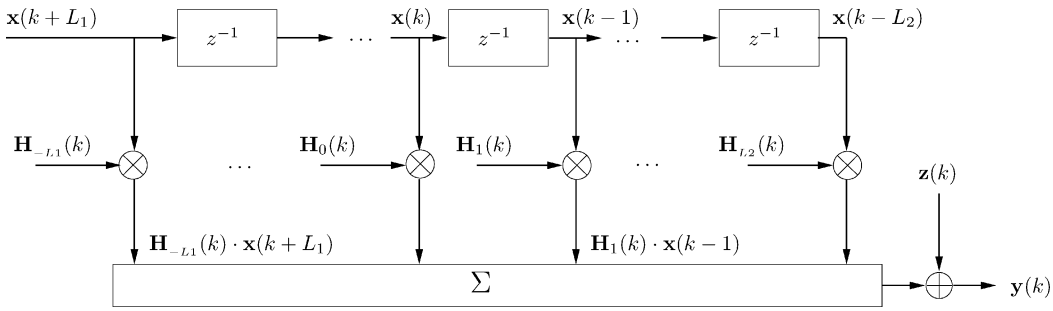

Fig. 2. Equivalent discrete-time MIMO channel model.

integers, and the total number of coefficients for the truncated FIR channel $h_{m,n}(k,l)$ is L with $L \le L_1+L_2+1$, where the equality is held if there are no discarded coefficients within the coefficient index range of $[-L_1, L_2]$.

Based on the above discussion and (6), we can now describe the input–output relationship of the MIMO channel in the discrete-time domain as follows:

$$\mathbf{y}(k) = \sum_{l=-L_1}^{L_2} \mathbf{H}_l(k)\cdot\mathbf{x}(k-l) + \mathbf{z}(k) \tag{10}$$

where $\mathbf{x}(k) = [x_1(k), x_2(k), \ldots, x_N(k)]^t$, $\mathbf{z}(k) = [z_1(k), z_2(k), \ldots, z_M(k)]^t$, and $\mathbf{y}(k) = [y_1(k), y_2(k), \ldots, y_M(k)]^t$ are the input vector, noise vector, and output vector at time instant k, respectively, with $(\cdot)^t$ being the transpose operator; $\mathbf{H}_l(k)$ is the lT_s delayed channel matrix at time instant k and defined by

$$\mathbf{H}_l(k) = \begin{bmatrix} h_{1,1}(k,l) & \cdots & h_{1,N}(k,l) \\ \vdots & \ddots & \vdots \\ h_{M,1}(k,l) & \cdots & h_{M,N}(k,l) \end{bmatrix}. \tag{11}$$

The block diagram of this discrete-time MIMO channel model is shown in Fig. 2.

It is noted that there are (MNL) stochastic channel coefficients, and an M-element random noise vector in this MIMO Rayleigh fading model (10). Since all of them are complex-valued Gaussian random variables, the first-order and second-order statistics of the channel coefficients and the noise vector will be sufficient to fully characterize the MIMO channel. For the convenience of discussion, we define the MIMO channel coefficient vector $\mathbf{h}_{vec}(k)$ as follows:

$$\mathbf{h}_{vec}(k) = [\mathbf{h}_{1,1}(k), \ldots, \mathbf{h}_{1,N}(k) \mid \cdots \mid \mathbf{h}_{M,1}(k), \ldots, \mathbf{h}_{M,N}(k)]^t \tag{12}$$

where $\mathbf{h}_{m,n}(k)$ is the (m,n)th subchannel's FIR coefficients at time k given by

$$\mathbf{h}_{m,n}(k) = [h_{m,n}(k,-L_1)\cdots h_{m,n}(k,L_2)]. \tag{13}$$

We are now ready to discuss the statistical properties of the MIMO channel.

B. Statistical Properties of the Discrete-Time Channel

Proposition 1: The noise vector $\mathbf{z}(k)$ is zero-mean Gaussian distributed with auto-covariance matrix $\mathbf{R}_{\mathbf{zz}}(k_1-k_2)$ given by

$$\begin{aligned}\mathbf{R}_{\mathbf{zz}}(k_1-k_2) &= E\left[\mathbf{z}(k_1)\cdot\mathbf{z}^h(k_2)\right] \\ &= N_0\cdot R_{p_R p_R}[(k_1-k_2)T_s]\cdot\mathbf{I}_M\end{aligned} \tag{14}$$

where $(\cdot)^h$ stands for the Hermitian of a complex-valued vector or matrix, $R_{p_R p_R}(\xi)$ is the auto-correlation function of the receive filter $p_R(t)$, N_0 is the two-sided power spectral density of the complex-valued additive white Gaussian noise (AWGN) $v_m(t)$, and $\mathbf{I}_M$ is an $M\times M$ identity matrix.

Proof: Since $z_m(t)$ is the output of a time-invariant linear filter with the input of zero-mean AWGN $v_m(t)$, $z_m(t)$ and its sampled version $z_m(kT_s)$ are both zero-mean Gaussian random variables. Noting that the zero-mean AWGN $v_m(t)$ is independent from time to time and from antenna to antenna (i.e., $E\left[v_{m_1}(t_1)v^*_{m_2}(t_2)\right] = N_0\delta(m_1-m_2)\delta(t_1-t_2)$) we can immediately get (14).

If the autocorrelation function of the receive filter $p_R(t)$ satisfies the following condition:

$$R_{p_R p_R}(kT_s) = 0, \quad k\neq 0 \tag{15}$$

then the discrete-time Gaussian noise $z_m(k)$ is still white, from sample to sample and from antenna to antenna, with variance of N_0 due to the receive filter being normalized to have energy of unity (i.e., $R_{p_R p_R}(0)=1$).

$$c(l_1,l_2) = \begin{cases} \int_{-\infty}^{+\infty} \bar{R}_{p_T p_R}(l_1T_s-\tau)\bar{R}^*_{p_T p_R}(l_2T_s-\tau)G(\tau)d\tau, & \text{if } G(\tau) \text{ is continuous} \\ \sum_{i=1}^{K}\sigma_i^2\bar{R}_{p_T p_R}(l_1T_s-\tau_i)\bar{R}^*_{p_T p_R}(l_2T_s-\tau_i), & \text{if } G(\tau) \text{ is given by (8)} \end{cases} \tag{17}$$

Proposition 2: The channel coefficients $h_{m,n}(k,l)$ and $h_{p,q}(k,l)$ are zero-mean Gaussian random variables, and their covariance function is given by

$$E\left[h_{m,n}(k_1,l_1)\cdot h^*_{p,q}(k_2,l_2)\right] = \rho_{Rx}^{(m,p)}\cdot\rho_{Tx}^{(n,q)}\cdot c(l_1,l_2)\cdot J_0\left[2\pi f_d(k_1-k_2)T_s\right] \quad (16)$$

where we have (17), as shown at the bottom of the previous page, with $\bar{R}_{p_Tp_R}(\xi)$ being the convolution function of the transmit filter and receive filter.

Proof: Based on (1) and $g_{m,n}(t,\tau)$ being zero-mean Gaussian processes, it is easy to conclude that $h_{m,n}(k,l)$ and $h_{p,q}(k,l)$ are zero-mean Gaussian random variables. Since $h_{m,n}(k,l)$ is the sampled version of $h_{m,n}(t,\tau)$, we have

$$h_{m,n}(k,l) = \int_{-\infty}^{+\infty} \bar{R}_{p_Tp_R}(lT_s-\tau)g_{m,n}(kT_s,\tau)d\tau. \quad (18)$$

According to Assumption 2, we can obtain (19), as shown at the bottom of the page, where $c(l_1,l_2)$ is given by (17). Thus, the proof is complete.

We are now in a position to present the statistical property of the channel coefficient vector $\mathbf{h}_{vec}(k)$ with the following theorem.

Theorem 1: The channel coefficient column vector $\mathbf{h}_{vec}(k)$ is zero-mean Gaussian distributed, its covariance matrix is given by

$$\begin{aligned}\mathbf{C}_{\mathbf{h}}(k_1-k_2) &= E\left\{\mathbf{h}_{vec}(k_1)\cdot\mathbf{h}^h_{vec}(k_2)\right\}\\ &= (\mathbf{\Psi}_{Rx}\otimes\mathbf{\Psi}_{Tx}\otimes\mathbf{C}_{\mathrm{ISI}})\cdot J_0\left[2\pi f_d(k_1-k_2)T_s\right]\end{aligned} \quad (20)$$

where $\otimes$ denotes the Kronecker product [27] and $\mathbf{C}_{\mathrm{ISI}}$ is the covariance matrix of the intersymbol interference (ISI) filter tap vector $\mathbf{h}_{m,n}(k)$. Likewise, $\mathbf{\Psi}_{Rx}$, $\mathbf{\Psi}_{Tx}$, and $\mathbf{C}_{\mathrm{ISI}}$ are given by

$$\mathbf{\Psi}_{Rx} = \begin{bmatrix} \rho_{Rx}^{(1,1)} & \cdots & \rho_{Rx}^{(1,M)} \\ \vdots & \ddots & \vdots \\ \rho_{Rx}^{(M,1)} & \cdots & \rho_{Rx}^{(M,M)} \end{bmatrix}$$

$$\mathbf{\Psi}_{Tx} = \begin{bmatrix} \rho_{Tx}^{(1,1)} & \cdots & \rho_{Tx}^{(1,N)} \\ \vdots & \ddots & \vdots \\ \rho_{Tx}^{(N,1)} & \cdots & \rho_{Tx}^{(N,N)} \end{bmatrix} \quad (21)$$

$$\mathbf{C}_{\mathrm{ISI}} = \begin{bmatrix} c(-L_1,-L_1) & \cdots & c(-L_1,L_2) \\ \vdots & \ddots & \vdots \\ c(L_2,-L_1) & \cdots & c(L_2,L_2) \end{bmatrix} \quad (22)$$

with $c(l_1,l_2)$ being determined by (17).

Proof: Based on (13), (16), and (17), we can immediately get

$$E\left[\mathbf{h}^t_{m,n}(k_1)\cdot\mathbf{h}^*_{p,q}(k_2)\right] = \rho_{Rx}^{(m,p)}\cdot\rho_{Tx}^{(n,q)}\cdot\mathbf{C}_{\mathrm{ISI}}\cdot J_0\left[2\pi f_d(k_1-k_2)T_s\right]. \quad (23)$$

According to (12) of the column vector $\mathbf{h}_{vec}(k)$, we can further get its covariance matrix as in (24), shown at the bottom of the page.

This completes the proof of the theorem.

C. Generation of the Discrete-Time MIMO Channel Fading

Having analyzed the statistical properties of the discrete-time MIMO channel model, we can generate the stochastic fading channel coefficients represented by the channel vector $\mathbf{h}_{vec}(k)$,

$$\begin{aligned}E\left[h_{m,n}(k_1,l_1)h^*_{p,q}(k_2,l_2)\right] &= \rho_{Rx}^{(m,p)}\cdot\rho_{Tx}^{(n,q)}\cdot J_0\left[2\pi f_d(k_1-k_2)T_s\right]\\ &\quad\times\int_{-\infty}^{+\infty}\int_{-\infty}^{+\infty}\bar{R}_{p_Tp_R}(l_1T_s-\tau)\bar{R}^*_{p_Tp_R}(l_2T_s-\mu)G(\tau)\delta(\tau-\mu)d\tau d\mu\\ &= \rho_{Rx}^{(m,p)}\cdot\rho_{Tx}^{(n,q)}\cdot J_0\left[2\pi f_d(k_1-k_2)T_s\right]\cdot c(l_1,l_2)\end{aligned} \quad (19)$$

$$\begin{aligned}\mathbf{C}_{\mathbf{h}}(k_1-k_2) &= \begin{bmatrix} \rho_{Rx}^{(1,1)}\rho_{Tx}^{(1,1)}\mathbf{C}_{\mathrm{ISI}} & \cdots & \rho_{Rx}^{(1,1)}\rho_{Tx}^{(1,N)}\mathbf{C}_{\mathrm{ISI}} & & \rho_{Rx}^{(1,M)}\rho_{Tx}^{(1,1)}\mathbf{C}_{\mathrm{ISI}} & \cdots & \rho_{Rx}^{(1,M)}\rho_{Tx}^{(1,N)}\mathbf{C}_{\mathrm{ISI}} \\ \vdots & \vdots & \vdots & \ddots & \vdots & \vdots & \vdots \\ \rho_{Rx}^{(1,1)}\rho_{Tx}^{(N,1)}\mathbf{C}_{\mathrm{ISI}} & \cdots & \rho_{Rx}^{(1,1)}\rho_{Tx}^{(N,N)}\mathbf{C}_{\mathrm{ISI}} & & \rho_{Rx}^{(1,M)}\rho_{Tx}^{(N,1)}\mathbf{C}_{\mathrm{ISI}} & \cdots & \rho_{Rx}^{(1,M)}\rho_{Tx}^{(N,N)}\mathbf{C}_{\mathrm{ISI}} \\ & \ddots & & \ddots & & \ddots & \\ \rho_{Rx}^{(M,1)}\rho_{Tx}^{(1,1)}\mathbf{C}_{\mathrm{ISI}} & \cdots & \rho_{Rx}^{(M,1)}\rho_{Tx}^{(1,N)}\mathbf{C}_{\mathrm{ISI}} & & \rho_{Rx}^{(M,M)}\rho_{Tx}^{(1,1)}\mathbf{C}_{\mathrm{ISI}} & \cdots & \rho_{Rx}^{(M,M)}\rho_{Tx}^{(1,N)}\mathbf{C}_{\mathrm{ISI}} \\ \vdots & \vdots & \vdots & \ddots & \vdots & \vdots & \vdots \\ \rho_{Rx}^{(M,1)}\rho_{Tx}^{(N,1)}\mathbf{C}_{\mathrm{ISI}} & \cdots & \rho_{Rx}^{(M,1)}\rho_{Tx}^{(N,N)}\mathbf{C}_{\mathrm{ISI}} & & \rho_{Rx}^{(M,M)}\rho_{Tx}^{(N,1)}\mathbf{C}_{\mathrm{ISI}} & \cdots & \rho_{Rx}^{(M,M)}\rho_{Tx}^{(N,N)}\mathbf{C}_{\mathrm{ISI}} \end{bmatrix}\\ &\quad\times J_0\left[2\pi f_d(k_1-k_2)T_s\right]\\ &= \begin{bmatrix} \rho_{Rx}^{(1,1)}\mathbf{\Psi}_{Tx} & \cdots & \rho_{Rx}^{(1,M)}\mathbf{\Psi}_{Tx} \\ \vdots & \vdots & \vdots \\ \rho_{Rx}^{(M,1)}\mathbf{\Psi}_{Tx} & \cdots & \rho_{Rx}^{(M,M)}\mathbf{\Psi}_{Tx} \end{bmatrix}\otimes\mathbf{C}_{\mathrm{ISI}}\cdot J_0\left[2\pi f_d(k_1-k_2)T_s\right]\\ &= (\mathbf{\Psi}_{Rx}\otimes\mathbf{\Psi}_{Tx}\otimes\mathbf{C}_{\mathrm{ISI}})\cdot J_0\left[2\pi f_d(k_1-k_2)T_s\right]\end{aligned} \quad (24)$$

whose covariance matrix matches the theoretical one given by Theorem 1 for computer simulations of MIMO systems.

Theorem 2: The zero-mean time-varying Rayleigh fading channel vector $\mathbf{h}_{vec}(k)$ can be generated by

$$\mathbf{h}_{vec}(k) = \mathbf{C_h}^{1/2}(0) \cdot \mathbf{\Phi}(k) = \left(\mathbf{\Psi}_{Rx}^{1/2} \otimes \mathbf{\Psi}_{Tx}^{1/2} \otimes \mathbf{C}_{\mathrm{ISI}}^{1/2}\right) \cdot \mathbf{\Phi}(k) \tag{25}$$

where $\mathbf{X}^{1/2}$ is the square root of matrix $\mathbf{X} = \mathbf{X}^{1/2} \cdot \left(\mathbf{X}^{1/2}\right)^h$, which can be obtained by a few methods shown in [28]; $\mathbf{\Phi}(k)$ is an $(MNL) \times 1$ vector, whose elements are uncorrelated Rayleigh flat fading, and

$$E\left[\mathbf{\Phi}(k_1) \cdot \mathbf{\Phi}^h(k_2)\right] = J_0\left[2\pi f_d(k_1 - k_2)T_s\right] \cdot \mathbf{I}_{MNL \times MNL}.$$

Proof: This theorem can be proved by using two identities of matrices [27]: $[A \otimes B]\,[C \otimes D] = [AC] \otimes [BD]$ and $[A \otimes B]^h = A^h \otimes B^h$, where the matrices have appropriate dimensions. Details are omitted here for brevity.

The significance of Theorem 2 is that it indicates that the generation of the stochastic channel coefficients of a MIMO system can be done through the Kronecker product of the square roots of three small matrices in the sizes of $M \times M$, $N \times N$, and $L \times L$, rather than the square root of a very large matrix $\mathbf{C_h}(0)$ in the size of $(MNL) \times (MNL)$. The number of operations required for the square root decomposition of $\mathbf{C_h}(0)$ is approximately $6M^3N^3L^3$ [28]. Alternatively, the number of operations required to decompose three smaller matrices is approximately $6(M^3 + N^3 + L^3)$, and the Kronecker product of the three matrices requires about $(M^2N^2L^2)/2$ operations. Therefore, the ratio between the number of operations of decomposing one large matrix and the number of operations to decompose three smaller matrices can be approximated by $12M^3N^3L^3/(12(M^3 + N^3 + L^3) + M^2N^2L^2)$. It is apparent that a significant amount of computations will be saved by this method, and it will additionally lead to much better numerical computation accuracy.

The generation of multiple uncorrelated Rayleigh flat fades is a classic topic with new challenges for the number (MNL) of multiple fades being large. It has been commonly postulated in the literature [6], [16], [17] that it can be done by Jakes' original simulator [29]. Unfortunately, there are two problems in the original Jakes' simulator. First, Jakes' simulator is a deterministic model, it has difficulty [30] in directly generating three or more uncorrelated Rayleigh flat fading waveforms. Secondly, and more importantly, it was shown in [31] that Jakes' simulator is even not stationary in the wide sense, and an improved Jakes' simulator was proposed in [31] to remove the stationarity problem. However, the improved Jakes' simulator along with the original Jakes' simulator have statistic deficiencies as pointed out in [32], and these statistic deficiencies were finally removed by new Rayleigh fading models developed in [33] and [34]. These new models can be employed for the generation of the multiple uncorrelated Rayleigh flat fading vector $\mathbf{\Phi}(k)$.

D. Computational Complexity

Theorems 1 and 2 imply that our discrete-time MIMO channel model is statistically equivalent to the conventional continuous-time channel model. In this section, we will show that the computational complexity of our proposed discrete-time MIMO channel simulation model is much lower than that of the conventional continuous-time simulation model, based on the following three aspects.

TABLE I
COMPUTATIONAL COMPLEXITY RATIO OF THE PROPOSED DISCRETE-TIME MODEL TO THE CONVENTIONAL CONTINUOUS-TIME MODEL

Profiles	TU	HT	EQ	PedA	PedB	VehA	VehB
ζ_γ	2.7%	2.7%	2.7%	3.8%	7.7%	3.8%	7.7%
ζ_L	66.7%	83.3%	100%	50%	100%	83.3%	100%
$\zeta < \zeta_\gamma\zeta_L$	1.8%	2.3%	2.7%	1.9%	7.7%	3.2%	7.7%

First, the sampling rate of the discrete-time model is $1/T_s$, which is equal to η/T_{sym} with η being a small positive integer. However, for the conventional continuous-time model, when the differential delay of multiple fading paths is very small compared to the symbol period T_{sym}, the sampling rate for simulation needs to be very high to implement the multiple fading paths. Let η_c/T_{sym} be the sampling rate for the continuous-time model, then the sampling computational complexity ratio of the discrete-time model to the continuous-time models is given by

$$\zeta_\eta = \frac{\eta}{\eta_c} \times 100\%. \tag{29}$$

Since η_c is usually much larger than η, the ratio ζ_η is usually very small. For channels with continuous power delay profile, such as the exponential power delay profile [13], a much higher η_c is required for continuous-time model, which will lead to an even smaller ζ_η.

Second, the number of uncorrelated fades used in the discrete-time model L_d is not larger than the number of uncorrelated fades used in the continuous-time model L_c. Thus the ratio $\zeta_L = (L_d/L_c) \times 100\%$ is not larger than one.

Third, for the discrete-time model, the effects of the transmit and receive filters are incorporated in the statistical channel coefficients with no additional filtering calculations involved. However, the simulation of the continuous-time model must pass the input signals through the transmit and receive filters with extra computations. Moreover, to represent the small differential delay of multiple fading paths, the continuous-time model has to use a high sampling rate which makes the transmit and receive filters have large number of taps. This makes the computational complexity of the continuous-time model even higher than that of the discrete-time model. Unfortunately, an explicit ratio between these two models is unlikely to be obtained.

Combining the aforementioned three facts, we can obtain the total computational complexity ratio of the discrete-time model to the continuous-time model as follows:

$$\zeta < \zeta_\eta\zeta_L. \tag{30}$$

For convenient comparison, Table I shows the computational complexity ratios for TU, HT, and EQ propagation profiles of EDGE system, and Pedestrian A (PedA), Pedestrian B (PedB), Vehicular A (VehA), and Vehicular B (VehB) propagation profiles of cdma2000 and UMTS systems. It is noted that these

profiles are commonly used simulation test cases for wireless system evaluation. As can be seen from the table, the newly proposed discrete-time MIMO channel model has much smaller computational complexity compared to the conventional continuous-time MIMO channel model.

IV. Simulation Experiments

In this section, we are going to evaluate the discrete-time MIMO channel model by simulation in three different criteria. First, we assess the statistic accuracy of the model compared to its theoretically calculated statistics. Second, we demonstrate the statistical equivalence between the proposed discrete-time model and the conventional continuous-time model through BER comparison. Third, we present the application of the model for MIMO channel capacity evaluation of a system which experiences triply selective Rayleigh fading.

A. Spatial–Temporal Statistics

Consider a MIMO system consisting of two antennas at the base station as the transmitter and two antennas at the mobile station as the receiver, then the correlation coefficient matrices $\mathbf{\Psi}_{Tx}$ and $\mathbf{\Psi}_{Rx}$ can be calculated by the formulas derived in [4] under certain spatial parameters. For example, if the BS and MS antennas are spaced by 12λ and 0.5λ, respectively, where λ is the wavelength, the angle of arrival is 90° and the angular spread is 10° as shown in Fig. 3, then we get the two matrices as follows:

$$\mathbf{\Psi}_{Tx} = \begin{bmatrix} 1.0000 & 0.2154 \\ 0.2154 & 1.0000 \end{bmatrix}, \mathbf{\Psi}_{Rx} = \begin{bmatrix} 1.0000 & -0.3042 \\ -0.3042 & 1.0000 \end{bmatrix}. \tag{31}$$

The power delay profile is exponentially decaying [13], [17] and given by $G(\tau) = A \cdot \exp(\tau/\mu s)$ for $0 \le \tau \le 5$ μs, and $G(\tau) = 0$ otherwise. Likewise, if the transmit filter is a linearized Gaussian filter with a time-bandwidth product 0.3 [35], the receive filter is a square root raised cosine (SRC) filter with a roll-off factor 0.3, and the sampling period T_s is 3.69 μs, then the elements $c(l_1, l_2)$ of the matrix $\mathbf{C}_{\text{ISI}}$ obtained by (17) are shown in Table II.

Having obtained the above three matrices, we can now compare the theoretical statistics as defined in (20) of the discrete-time MIMO fading channel coefficients with their corresponding empirical correlations obtained from simulations. For illustration purposes, we only show three of the comparisons here. Based on Theorem 1, the theoretical autocorrelation (same as the auto-covariance for a zero mean random variable) function of the channel coefficient $h_{1,1}(k,1)$ is given by $0.5583 \times J_0[2\pi f_d(k_1 - k_2)T_s]$, the theoretical cross-correlation function of the channel coefficients $h_{1,1}(k,0)$ and $h_{1,1}(k,1)$ is given by $0.3407 \times J_0[2\pi f_d(k_1 - k_2)T_s]$, and the theoretical cross-correlation function of the channel coefficients $h_{1,1}(k,0)$ and $h_{2,1}(k,1)$ is given by $-0.1036 \times J_0[2\pi f_d(k_1 - k_2)T_s]$. Using the procedure described in Section III-C, we have generated a set of the time-varying random channel coefficients for $h_{1,1}(k,0)$, $h_{1,1}(k,1)$, and $h_{2,1}(k,1)$. Then, their correlation statistics obtained from the simulation are compared to their corresponding theoretical ones and depicted in Fig. 4. As can be seen, the spatio-temporal statistics of the MIMO channel simulation model match the theoretical results very well. We

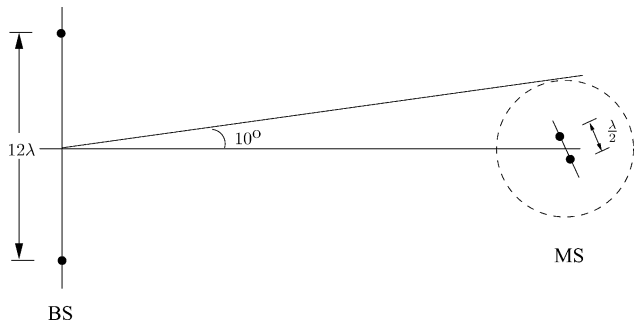

Fig. 3. Antenna placement of the 2×2 MIMO system.

TABLE II
Matrix $\mathbf{C}_{\text{ISI}}$ for the Exponential Delay Power Profile

$c(l_1, l_2)$	$l_2 = -1$	$l_2 = 0$	$l_2 = 1$	$l_2 = 2$
$l_1 = -1$	0.0091	0.0426	0.0178	-0.0016
$l_1 = 0$	0.0426	0.3664	0.3407	0.0367
$l_1 = 1$	0.0178	0.3407	0.5583	0.1414
$l_1 = 2$	-0.0016	0.0367	0.1414	0.0602

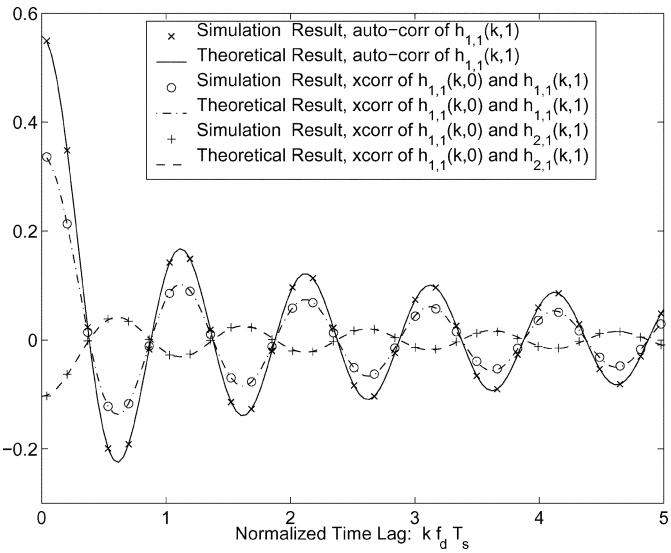

Fig. 4. Comparison of the theoretically calculated and empirically simulated auto-correlation of $h_{1,1}(k,1)$, cross correlation of $h_{1,1}(k,0)$ and $h_{1,1}(k,1)$, and cross correlation of $h_{1,1}(k,0)$ and $h_{2,1}(k,1)$.

have also compared the correlation statistics of all other channel coefficients to their theoretical ones, finding good agreement in all cases. Therefore, the statistical accuracy of the the discrete-time MIMO channel model is confirmed.

We conclude this subsection with two remarks. First, the nonzero cross correlations between $h_{1,1}(k,0)$ and $h_{1,1}(k,1)$ and between $h_{1,1}(k,0)$ and $h_{2,1}(k,1)$ indicate that the fading coefficients from different subchannels with different delays can be statistically correlated (or even significantly correlated sometimes). This is quite different from the commonly used independence assumption in the literature [6], [36], [37], where the transmit and receive filters were not taken into consideration. Second, the conventional continuous-time channel model needs a very high oversampling rate [13] to approximately

TABLE III
MATRIX $\mathbf{C}_{\text{ISI}}$ FOR THE REDUCED SIX-PATH TU PROFILE

$c(l_1, l_2)$	$l_2 = -1$	$l_2 = 0$	$l_2 = 1$	$l_2 = 2$	$l_2 = 3$
$l_1 = -1$	0.0481	0.1799	0.0678	-0.0030	0.0029
$l_1 = 0$	0.1799	0.7401	0.3253	-0.0073	0.0121
$l_1 = 1$	0.0678	0.3253	0.1957	0.0168	0.0052
$l_1 = 2$	-0.0030	-0.0073	0.0168	0.0133	-0.0002
$l_1 = 3$	0.0029	0.0121	0.0052	-0.0002	0.0002

simulate this continuous power delay profile $G(\tau)$, but our discrete-time channel model can efficiently and accurately simulate the continuous delay power profile, as shown earlier.

B. BER Comparison

The statistical equivalence of the discrete-time channel model to the conventional continuous-time channel model can be demonstrated by comparing their BER performances. We choose the EDGE system [22], [35], as an example in this section. The power delay profile $G(\tau)$ used here is the reduced six-path TU profile provided in [22] with of all the six paths characterized by uncorrelated Rayleigh flat fading as specified. The transmit filter, receiver filter, and sampling period are the same as those used in the last section. The matrix $\mathbf{C}_{\text{ISI}}$ is given in Table III. It should be pointed out from this table that the power of this discrete-time channel is mainly concentrated on $h(k, 0)$ and $h(k, 1)$, corresponding to the values of $c(0, 0)$ and $c(1, 1)$, respectively. The total power of this truncated discrete-time channel is, given by the trace of $\mathbf{C}_{\text{ISI}}$, 0.9975, which is slightly less than unity as expected.

It is also noted that the SRC receive filter satisfies (15), so the additive noise in the discrete-time channel is still AWGN and can be directly generated by computer simulations. Assuming perfect channel estimation at the receiver for both the discrete-time channel model and continuous-time channel model, and by employing MLSE with the Viterbi algorithm for channel equalization with truncated channel memory length 4, we have obtained the uncoded BER versus E_b/N_0 shown in Fig. 5.

Apparently, the BER performance of the discrete-time channel model is almost identical to that of the continuous-time channel model. This demonstrates that the discrete-time channel model is statistically equivalent to the continuous-time channel model. However, according to Table I, the discrete-time model needs only about 1.8% computations of the continuous-time model to generate the statistical fading channel coefficients in this SISO example. This computational saving is very significant for discrete-time MIMO channels, where the computational burden for the generation of MIMO channel fading is a big issue.

C. MIMO Channel Capacity

In this section, the MIMO channel capacity is evaluated, using our discrete-time channel model, for triply selective Rayleigh fading channels to indicate the effects of spatial correlations, multipaths, and number of antennas on the channel capacity.

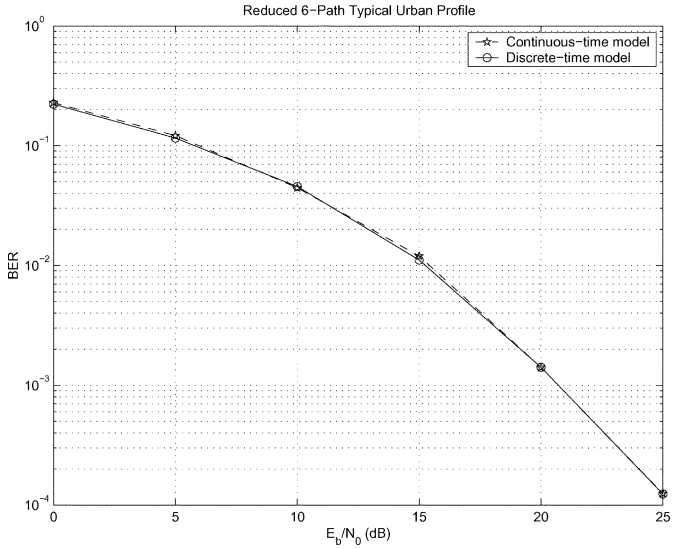

Fig. 5. Comparison of BER performance with discrete-time model and continuous-time model for EDGE mobile system under typical urban delay power profile.

When the MIMO channel is known to the receiver but unknown to the transmitter and assuming that the available power is uniformly distributed over all the transmit antennas, then the capacity of a spatially correlated MIMO WSSUS multipath Rayleigh channel with fixed total transmission power P_T is given by [38]

$$C = \frac{1}{2W} \times \int_{-W}^{W} \log_2 \det \left[\mathbf{I}_M + \frac{\beta}{N} \cdot \mathbf{H}(k, f) \cdot \mathbf{H}^h(k, f) \right] df, \ \frac{\text{bps}}{\text{Hz}} \tag{32}$$

where W is the one-sided bandwidth of the baseband signal, β is the average signal-to-noise (SNR) at each receiver branch, and $\mathbf{H}(k, f)$ is the time-varying frequency-dependent transfer function matrix given by

$$\mathbf{H}(k, f) = \sum_{l=-L_1}^{L_2} \mathbf{H}_l(k) z^{-l} \Big|_{z=\exp(j2\pi f T_s)}. \tag{33}$$

Obviously, the channel capacity C is a function of $\mathbf{H}(k, f)$, which is random for each channel realization. Hence, C can be treated as a random variable. The outage capacity, which is defined as the probability that a specified value of C cannot be achieved, is used to evaluate the capacity of the channel. It can be represented by the complementary cumulative distribution function (ccdf) of the random capacity C.

We take the UMTS system as an example. The power delay profile is chosen to be the vehicular channel A profile specified in [23]. The transmit and receive filters are SRC filters with rolloff factor 0.22, and the sampling period is the same as the chip period 0.260 42 μs [23]. The matrix $\mathbf{C}_{\text{ISI}}$ can be calculated based on (22), but details are omitted here for brevity. For the convenience of illustration purposes, the elements of the correlation coefficient matrices $\mathbf{\Psi}_{Tx}$ and $\mathbf{\Psi}_{Rx}$ are simply chosen to be exponential correlation matrix [39] as follows:

$$\rho_{Rx}^{(m,p)} = r^{|m-p|}, \ \rho_{Tx}^{(n,q)} = r^{|n-q|}, \ |r| \leq 1. \tag{34}$$

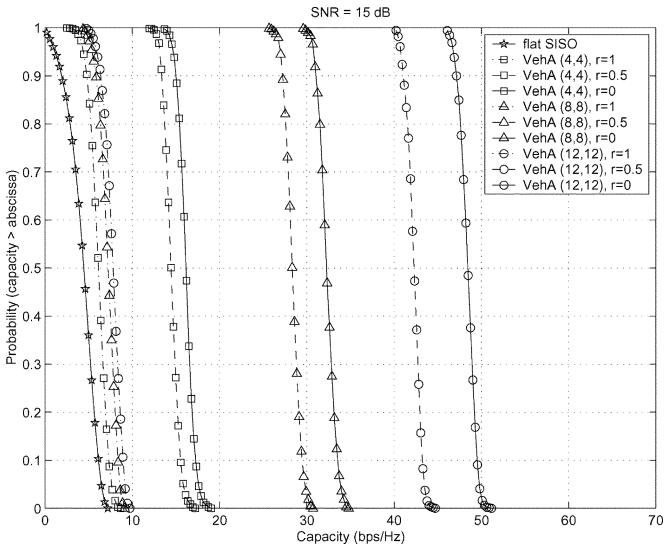

Fig. 6. Capacities of MIMO channels with different spatial correlation coefficients and $M = N$. Dashed-dotted lines stand for $r = 1$, dashed lines for $r = 0.5$, and solid lines for $r = 0$. Channel capacity is linearly scaling with M when $r \leq 0.5$, and the scaling rate is dependent on the value of r.

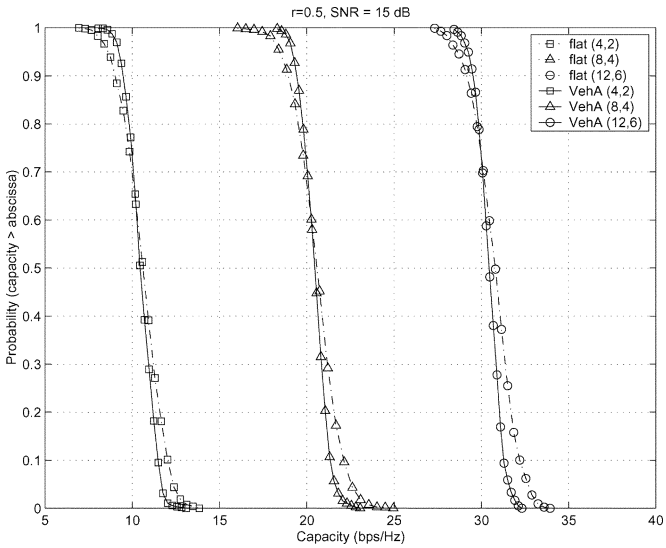

Fig. 7. Capacities of MIMO channels with different delay power profiles, M-to-N ratio being constant and $r = 0.5$. Channel capacity is linearly scaling with M.

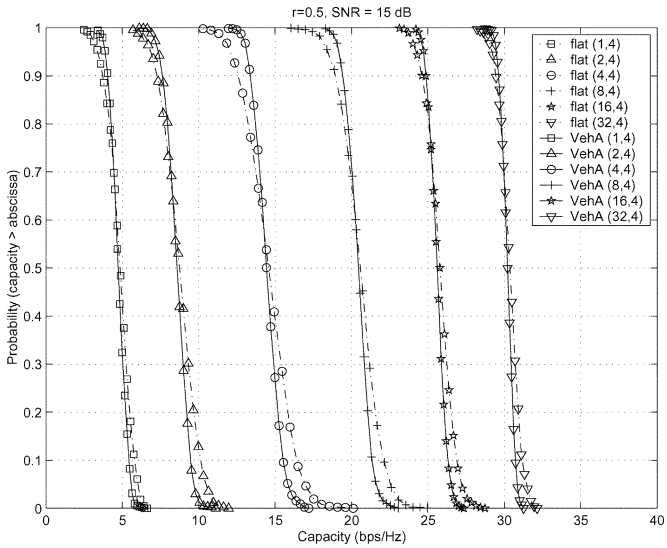

Fig. 8. Capacities of MIMO channels with N being fixed. Dashed-dotted lines stand for flat fading, solid lines for vehicular channel A profile. Channel capacity is approximately linearly scaling with $\log_2 M$ when $M \geq N$.

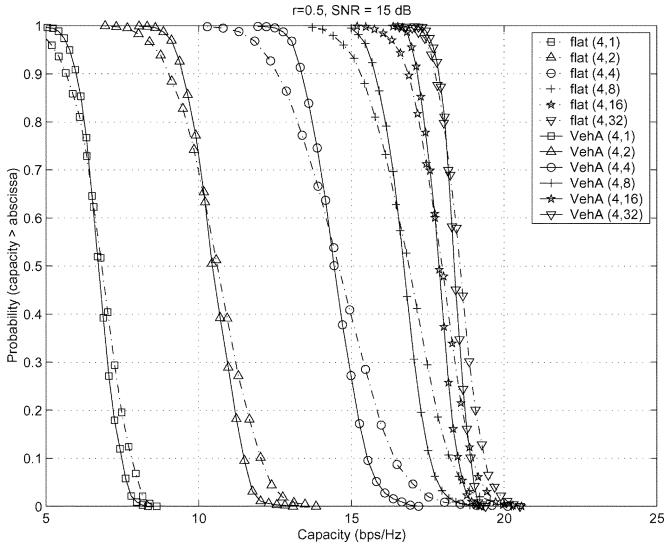

Fig. 9. Capacities of MIMO channels with M being fixed. Dashed-dotted lines stand for flat fading, solid lines for vehicular channel A profile. Channel capacity is linearly scaling with $\log_2 N$ when $N \leq M$.

The capacity ccdfs of MIMO channels under different correlation coefficients $r = 0, 0.5, 1.0$ and different number of antennas with $M = N$ are shown in Fig. 6, where the SISO flat fading channel is included for comparison purposes. It is noted that the number of receive antennas M and the number of transmit antennas N is indicated by (M, N) in the figure's legend. As can be seen, when $M = N$, the MIMO channel capacity is linearly growing with M when $r \leq 0.5$, and the growing rate depends on the value of r (the smaller r is, the larger the growth rate). This shows that the spatial correlation of the MIMO channel has a strong impact on the channel capacity. This observation for a frequency selective channel is in good agreement with the results presented in [24] for Rayleigh flat fading.

The capacity ccdfs of flat fading channels, and the vehicular A profile with M-to-N ratio being constant and $r = 0.5$ are plotted in Fig. 7 to compare the flat fading and frequency selective fading's impact on the channel capacity. As can be seen, for 10% or less outage capacity, i.e., the probability (capacity $>$ abscissa) ≥ 0.9, thus the frequency selective fading channels always have a larger capacity than the flat fading channels. This supports the view point that the rich scattering environment (multipath) provides higher channel capacity [38]. It is also observed that when $M \neq N$ but M/N is constant, the MIMO channel capacity is still linearly growing with M for both flat fading and frequency selective fading.

The capacity ccdf's of the flat fading channel and vehicular channel A profile with N being fixed and M being fixed are plotted in Figs. 8 and 9, respectively. It can be observed from Fig. 8 that the channel capacity is approximately linearly changing with $\log_2 M$ when $M \geq N$ and N is fixed. It can also be concluded from Fig. 9 that the channel capacity is linearly

changing with $\log_2 N$ when $N \leq M$ and M is fixed. It should be pointed out that the MIMO channel capacity results reported in [1], [2], and [40] are only for i.i.d. flat Rayleigh fading channels. Hence, our simulation results are valuable observations for triply selective MIMO Rayleigh fading channels.

Finally, it is noted that the MIMO channel capacity with continuous-time models has also been performed by extensive simulations, and the results are all nearly identical to those obtained with the discrete-time model. This further verifies the statistical equivalence of the discrete-time and continuous-time channel models. However, with the discrete-time MIMO channel model, the outage capacity for the MIMO channel can be easier and more efficiently evaluated.

V. Conclusion

We have proposed a new discrete-time channel model for MIMO systems over space-selective (or spatially correlated), time-selective (or time-varying), and frequency-selective Rayleigh fading channels, which are referred to as triply selective Rayleigh fading channels. The stochastic channel coefficients of the new MIMO channel model have the same sampling period as that of the MIMO receiver, and they can be efficiently generated from a new method, presented in this paper. The proposed approach combines the effects of the transmit filter, the physical MIMO channel multipath fading, and the receive filter. The new model is computationally efficient to describe the input–output of MIMO channels, because it does not need to oversample the fractionally delayed multipath channel fading, the transmit filter, and the receive filter. It is shown through analysis and simulation that the discrete-time stochastic channel coefficients of different individual subchannels with different delays are generally *statistically correlated* even if the physical channels have WSSUS multipath fading. The knowledge of this correlation may be used for improving the channel estimation of MIMO systems. The statistical accuracy of the discrete-time channel model is rigorously confirmed by extensive simulations in terms of second-order statistics and BER performance of a system that uses the model. The discrete-time MIMO channel model is further used to evaluate the MIMO channel capacity under a triply selective Rayleigh fading environment. For the high SNR scenario, from the simulation experiments, we have three observations: 1) when the number of receive antennas M is the same as the number of transmit antennas N, or when M/N is constant, the MIMO channel capacity vary in a linear fashion with M; 2) when N is fixed, the MIMO channel capacity increases approximately linearly with $\log_2 M$ when $M \geq N$; and 3) when M is fixed, the MIMO channel capacity is linearly scaling with $\log_2 N$ when $N \leq M$. However, the scaling rates for all the three cases are dependent on the spatial correlation coefficients (the less correlation, the larger the scaling rate). Our observations are therefore valuable extensions to the capacity results of triply selective MIMO Rayleigh fading channels from the special case of quasistatic i.i.d. flat Rayleigh fading MIMO channels.

Acknowledgment

The authors would like to thank the anonymous reviewers and the Editor, Dr. F. Zheng, for their careful reviews and valuable comments. The authors also wish to thank Dr. C. Sgraja for his helpful comments.

References

[1] I. E. Telatar, "Capacity of multi-antenna Gaussian channels," *Eur. Trans. Telecom.*, vol. 10, pp. 585–595, Nov. 1999.

[2] G. J. Foschini and M. J. Gans, "On limits of wireless communications in a fading environment when using multiple antennas," *Wireless Personal Commun.*, vol. 6, pp. 311–335, 1998.

[3] G. G. Raleigh and J. M. Cioffi, "Spatio-temporal coding for wireless communications," *IEEE Trans. Commun.*, vol. 46, pp. 357–366, Mar. 1998.

[4] D. S. Shiu, G. J. Foschini, M. J. Gans, and J. M. Kahn, "Fading correlation and its effect on the capacity of multielement antenna systems," *IEEE Trans. Commun.*, vol. 48, pp. 502–513, Mar. 2000.

[5] M. Stege, J. Jelitto, M. Bronzel, and G. Fettweis, "A multiple input – multiple output channel model for simulation of TX- and RX- diversity wireless systems," in *Proc. IEEE VTC Fall*, 2000, pp. 833–839.

[6] K. I. Pedersen, J. B. Andersen, J. P. Kermoal, and P. Mogensen, "A stochastic multiple-input-multiple-output radio channel model for evaluation of space-time coding algorithms," in *Proc. IEEE VTC Fall*, 2000, pp. 893–897.

[7] D. Gesbert, H. Bolcskei, D. A. Gore, and A. J. Paulraj, "MIMO wireless channels: Capacity and performance prediction," in *Proc. IEEE Globecom*, 2000, pp. 1083–1088.

[8] T. Svantesson, "A physical MIMO radio channel model for multi-element multi-polarized antenna systems," in *Proc. IEEE VTC Fall*, 2001, pp. 1083–1087.

[9] M. Steinbauer, A. F. Molisch, and E. Bonek, "The double-directional radio channel," *IEEE Antennas Propagat. Mag.*, vol. 43, pp. 51–63, Aug. 2001.

[10] G. German, Q. Spencer, L. Swindlehurst, and R. Valenzuela, "Wireless indoor channel modeling: Statistical agreement of ray tracing simulations and channel sounding measurements," in *Proc. IEEE ICASSP*, 2001, pp. 2501–2504.

[11] A. M. Sayeed, "Modeling and capacity of realistic spatial MIMO channels," in *Proc. IEEE ICASSP*, 2001, pp. 2489–2492.

[12] J. P. Kermoal, L. Schumacher, K. I. Pedersen, P. E. Mogensen, and F. Frederiksen, "A stochastic MIMO radio channel model with experimental validation," *IEEE J. Select. Areas Commun.*, vol. 20, pp. 1211–1226, Aug. 2002.

[13] M. C. Jeruchim, P. Balaban, and K. S. Shanmugan, *Simulation of Communication Systems: Modeling, Methodology, and Techniques*, 2nd ed. Berlin, Germany: Kluwer, 2000.

[14] G. D. Forney, "Maximum-likelihood sequence estimation of digital sequences in the presence of intersymbol interference," *IEEE Trans. Inform. Theory*, vol. IT-18, pp. 363–378, May 1972.

[15] P. Hoeher, "A statistical discrete-time model for the WSSUS multipath channel," *IEEE Trans. Veh. Technol.*, vol. 41, pp. 461–468, 1992.

[16] K. W. Yip and T. S. Ng, "Efficient simulation of digital transmission over WSSUS channels," *IEEE Trans. Commun.*, vol. 43, pp. 2907–2913, Dec. 1995.

[17] ——, "Discrete-time model for digital communications over a frequency-selective Rician fading WSSUS channel," *Proc. Inst. Elec. Eng. Commun.*, vol. 143, pp. 37–42, Feb. 1996.

[18] P. A. Bello, "Characterization of randomly time-variant linear channels," *IEEE Trans. Commun. Syst.*, vol. 11, pp. 360–393, Dec. 1963.

[19] J. D. Parsons, *The Mobile Radio Propagation Channel*, 2nd ed. New York: Wiley, 2000.

[20] R. B. Ertel, P. Cardieri, K. W. Sowerby, T. S. Rappaport, and R. H. Reed, "Overview of spatial channel models for antenna array communication systems," *IEEE Personal Commun.*, pp. 10–21, Feb. 1998.

[21] R. D. Murch and K. B. Letaief, "Antenna systems for broadband wireless access," *IEEE Commun. Mag.*, vol. 40, pp. 76–83, Apr. 2002.

[22] "Radio Transmission and Reception," ETSI. GSM 05.05, ETSI EN 300 910 V8.5.1, 2000.

[23] "Selection procedure for the choice of radio transmission technologies of UMTS," UMTS, UMTS 30.03 version 3.2.0 ETSI, 1998.

[24] C. N. Chuah, D. N. C. Tse, J. M. Kahn, and R. A. Valenzuela, "Capacity scaling in MIMO wireless systems under correlated fading," *IEEE Trans. Inform. Theory*, vol. 48, pp. 637–650, Mar. 2002.

[25] S. Loyka and A. Kouki, "New compound upper bound on MIMO channel capacity," *IEEE Commun. Lett.*, vol. 6, pp. 96–98, Mar. 2002.

[26] A. Abdi and M. Kaveh, "A space-time correlation model for multielement antenna systems in mobile fading channels," *IEEE J. Select. Areas Commun.*, vol. 20, pp. 550–560, Apr. 2002.

[27] A. Graham, *Kronecker Products and Matrix Calculus: With Applications*: Wiley, 1981.
[28] G. H. Golub and C. F. Van Loan, *Matrix Computation*, 3rd ed. Baltimore, MD: Johns Hopkins Univ. Press, 1996.
[29] W. C. Jakes, *Microwave Mobile Communications*. Piscataway, NJ: IEEE Press, 1994.
[30] J. Han, C. Mun, and H. Park, "A deterministic fading channel model with rigorous correlation characteristics," in *Proc. IEEE VTC- Fall*, 1999, pp. 122–126.
[31] M. F. Pop and N. C. Beaulieu, "Limitations of sum-of-sinusoids fading channel," *IEEE Trans. Commun.*, vol. 49, pp. 699–708, Apr. 2001.
[32] C. Xiao, Y. R. Zheng, and N. C. Beaulieu, "Second-order statistical properties of the WSS Jakes' fading channel simulator," *IEEE Trans. Commun.*, vol. 50, pp. 888–891, June 2002.
[33] Y. R. Zheng and C. Xiao, "Improved models for the generation of multiple uncorrelated Rayleigh fading waveforms," *IEEE Commun. Lett.*, vol. 6, pp. 256–258, June 2002.
[34] ——, "Simulation models with correct statistical properties for Rayleigh fading channels," *IEEE Trans. Commun.*, vol. 51, pp. 920–928, June 2003.
[35] W. H. Gerstacker and R. Schober, "Equalization concepts for EDGE," *IEEE Trans. Wireless Commun.*, vol. 1, pp. 190–199, Jan. 2002.
[36] J. G. Proakis, *Digital Communications*, 4th ed. Upper Saddle River, NJ: McGraw-Hill, 2001.
[37] B. A. Bjerke and J. G. Proakis, "Equalization and decoding for multiple-input multiple-output wireless channels," *EURASIP J. Appl. Signal Processing*, vol. 2002, pp. 249–266, Mar. 2002.
[38] A. F. Molisch, M. Steinbauer, M. Toeltsch, E. Bonek, and R. S. Thoma, "Capacity of MIMO systems based on measured wireless channels," *IEEE J. Select. Areas Commun.*, vol. 20, pp. 561–569, Apr. 2002.
[39] S. L. Loyka, "Channel capacity of MIMO architecture using the exponential correlation matrix," *IEEE Commun. Lett.*, vol. 5, pp. 369–371, 2001.
[40] A. Grant, "Rayleigh fading multi-antenna channels," *EURASIP J. Appl. Signal Processing*, vol. 2002, pp. 316–329, Mar. 2002.

Chengshan Xiao (M'99–SM'02) received the B.S. degree from the University of Electronic Science and Technology of China, Chengdu, China, in 1987, the M.S. degree from Tsinghua University, Beijing, China, in 1989, and the Ph.D. degree from the University of Sydney, Sydney, Australia, in 1997, all in electrical engineering.

From 1989 to 1993, he was on the Research Staff and then became a Lecturer with the Department of Electronic Engineering at Tsinghua University. From 1997 to 1999, he was a Senior Member of Scientific Staff at Nortel Networks, Ottawa, ON, Canada. From 1999 to 2000, he was an Assistant Professor with the Department of Electrical and Computer Engineering at the University of Alberta, Edmonton, AB, Canada. Currently, he is an Assistant Professor with the Department of Electrical and Computer Engineering, University of Missouri, Columbia. His research interests include wireless communications, signal processing, and multidimensional and multirate systems. He has published extensively in these areas. Some of his algorithms have been implemented into Nortel's base station radios with successful technical field trials and network integration.

Dr. Xiao is an Associate Editor for the IEEE TRANSACTIONS ON WIRELESS COMMUNICATIONS, the IEEE TRANSACTIONS ON VEHICULAR TECHNOLOGY, the IEEE TRANSACTIONS ON CIRCUITS AND SYSTEMS-I, and the international journal of *Multidimensional Systems and Signal Processing*.

Jingxian Wu received the B.S.E.E. degree from Beijing University of Aeronautics and Astrophysics, Beijing, China, in 1998 and the M.S.E.E. degree from Tsinghua University, Beijing, in 2001. He is currently working toward the Ph.D. degree at University of Missouri, Columbia, in the Department of Electrical and Computer Engineering.

His research interests include the physical layers of wireless communication systems, including MIMO channel modeling, performance analysis of diversity systems, space-time coding, channel estimation and equalization, and spread spectrum communications.

Mr. Wu is a member of Tau Beta Pi.

Sang-Yick Leong received the B.S. and M.S.E.E. degrees from University of Missouri, Columbia, in 1999 and 2001, respectively. He is currently working toward the Ph.D. degree at the same institution in the Department of Electrical and Computer Engineering.

His research interests include the physical layers of wireless communications, such as MIMO channel modeling, capacity of MIMO mobile radio channel, space-time coding, channel estimation and equalization, and spread spectrum communications.

Yahong Rosa Zheng received the B.S. degree from the University of Electronic Science and Technology of China, Chengdu, China, in 1987, the M.S. degree from Tsinghua University, Beijing, China, in 1989, and the Ph.D. degree from Carleton University, Ottawa, ON, Canada, in 2002, all in electrical engineering.

From 1989 to 1994, she was a Senior Member of the Scientific Staff with Peony Electronic Group, Beijing. From 1994 to 1997, she held positions with GPS Solutions at Sagem Australasia Pty. Ltd., Sydney, Australia, and Polytronics Pty. Ltd., Toronto, Canada. Currently, she is an NSERC Postdoctoral Fellow with the Department of Electrical and Computer Engineering at the University of Missouri, Columbia. Her research interests include digital signal processing algorithms, array signal processing, channel estimation, and modeling for wireless communications. She has published a number of papers in international journals and conferences and has received two patents in China.

Khaled Ben Letaief (S'85–M'86–SM'97–F'03) received the B.S. degree *with distinction* and the M.S. and Ph.D. degrees in electrical engineering from Purdue University, West Lafayette, IN, in 1984, 1986, and 1990, respectively.

From January 1985 and as a Graduate Instructor in the School of Electrical Engineering at Purdue University, he has taught courses in communications and electronics. From 1990 to 1993, he was a Faculty Member at the University of Melbourne, Melbourne, Australia. Since 1993, he has been with the Hong Kong University of Science and Technology (HKUST), Kowloon, Hong Kong, where he is currently a Professor and Head of the Electrical and Electronic Engineering Department. He is also the Director of the Hong Kong Telecom Institute of Information Technology, as well as the Director of the Center for Wireless Information Technology. His current research interests include wireless and mobile networks, broadband wireless access, space–time processing for wireless systems, multiuser detection, wireless multimedia communications, and CDMA systems.

Dr. Letaief has been appointed the founding Editor-in-Chief of the IEEE TRANSACTIONS ON WIRELESS COMMUNICATIONS, in January 2002. He has served on the Editorial Board of other journals including the IEEE TRANSACTIONS ON COMMUNICATIONS, *IEEE Communications Magazine*, and IEEE JOURNAL ON SELECTED AREAS IN COMMUNICATIONS—Wireless Series (as Editor-in-Chief). He served as the Technical Program Chair of the 1998 *IEEE GLOBECOM Miniconference on Communications Theory*, held in Sydney, Australia. He was also the Co-Chair of the 2001 *IEEE ICC Communications Theory Symposium*, held in Helsinki, Finland. He is currently serving as the Chair of the IEEE Communications Society Technical Committee on Personal Communications. In addition to his active research activities, he has also been a dedicated teacher committed to excellence in teaching and scholarship. He received the Mangoon Teaching Award from Purdue University in 1990, the Teaching Excellence Appreciation Award by the School of Engineering at HKUST in Spring 1995, Fall 1996, Fall 1997, and Spring 1999, and the Michael G. Gale Medal for Distinguished Teaching (highest university-wide teaching award and only one recipient/year is honored for his/her contributions).